ELSEVIER

Journal of Luminescence 97 (2002) 107–114

JOURNAL OF LUMINESCENCE

www.elsevier.com/locate/jlumin

Site selective 4f5d spectroscopy of $CaF_2:Pr^{3+}$

K.D. Oskam, A.J. Houtepen, A. Meijerink*

Department of Condensed Matter, Debye Institute, Utrecht University, P.O. Box 80 000, 3508 TA Utrecht, Netherlands

Received 20 March 2001; received in revised form 15 August 2001; accepted 15 August 2001

Abstract

Spectroscopic investigations were performed on a single crystal of CaF_2 doped with 0.05% Pr^{3+}. Three different Pr^{3+} sites with different luminescent properties were identified. The $4f^2 \rightarrow 4f^15d^1$ excitation spectrum of the first site has a sharp maximum at 221.3 nm. Excitation in the 4f5d bands of this site yields strong 4f5d emissions in the UV/VIS part of the spectrum and also weaker intraconfigurational $4f^2$ emissions. By comparing the intraconfigurational 4f emissions and their decay times with data from the literature, these 4f5d bands are assigned to transitions on Pr^{3+} ions on a site with C_{4V} symmetry. The fd excitation spectrum of the second site has a zero phonon line at 223.3 nm. Upon selective excitation in this band, only 4f5d emission is observed. Probably, these 4f5d bands correspond to Pr^{3+} ions on a O_h site. The third set of 4f5d bands has a 4f5d onset at 208 nm. By comparison of the luminescence spectra of the intraconfigurational $4f^2$ transitions with literature data, these transitions are assigned to Pr^{3+} on an L site. Excitation in these 4f5d band yields $^1S_0$ emission followed by emission from the $^3P_0$ state. The present results clarify some contradictions reported in the literature.

Keywords: Luminescence spectroscopy; Lanthanides; Site selective spectroscopy; Vacuum ultraviolet; Pr^{3+}

1. Introduction

Currently, there is a large interest in luminescent compounds with visible quantum efficiencies larger than 100% upon irradiation with vacuum ultraviolet radiation (VUV, $\lambda < 200$ nm), see e.g. [1–6]. Such phosphors are called quantum cutters and can be applied to convert VUV radiation efficiently into visible light, for instance in mercury-free fluorescent tubes and plasma display panels. In both devices light emission is based on a xenon discharge, in which VUV radiation is generated. Up to now, a few compounds have been found that show visible quantum cutting (e.g. $LiGdF_4:Eu^{3+}$ [1,2] and $LiGdF_4:Er^{3+}$, Tb^{3+} [3]). Visible quantum cutting is accomplished in these substances via downconversion processes, in which energy transfer between different types of rare earth ions is involved. The first rare earth ion however for which visible quantum cutting was observed is Pr^{3+}. In 1974 it was observed by Sommerdijk et al. [7,8] and, independently, by Piper et al. [9] that $YF_3:Pr^{3+}$ has a visible quantum efficiency larger than 100% upon irradiation of this compound by VUV radiation. The mechanism

*Corresponding author. Tel: +31-30-253-2202; fax: +31-30-253-2403.

E-mail address: a.meijerink@phys.uu.nl (A. Meijerink).

0022-2313/02/$ - see front matter
PII: S0022-2313(01)00242-3

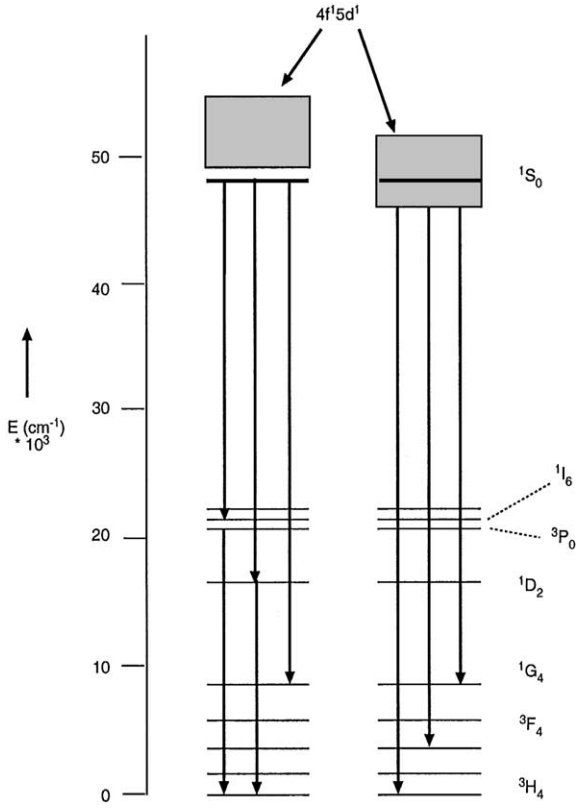

Fig. 1. Energy level scheme of Pr^{3+} showing the $4f^2$ levels and two situations for the position of the 4f5d levels. On the left the lowest 4f5d level is above the $^1S_0$ level making quantum cutting from the $^1S_0$ level possible. On the right the 4f5d level is situated below the $^1S_0$ level and mainly fd emission in the UV to the lower $4f^2$ levels is observed.

by which this phenomenon is explained is as follows (see also Fig. 1): in YF_3 the 4f5d levels of Pr^{3+} on a Y^{3+} site are situated at high energies, due to a low covalency of the ligands and a small crystal field. The onset of the 4f5d levels is higher in energy than the $^1S_0$ level, which is situated at about 47,000 cm^{-1}. After excitation of Pr^{3+} in the 4f5d levels (via a spin and parity allowed transition) nonradiative relaxation takes place to this $^1S_0$ level. From this level, different radiative transitions can occur to lower states, but the dominant one in YF_3 is the $^1S_0 \rightarrow {}^1I_6$ transition. Hereby, a photon with a wavelength of about 400 nm is emitted. From the $^1I_6$ level, nonradiative relaxation takes place to the $^3P_0$ level, from which a second photon can be emitted in the visible part of the spectrum (most intense lines are due to the $^3P_0 \rightarrow {}^3H_4$ and $^3P_0 \rightarrow {}^3F_2$ transitions). The overall visible quantum efficiency of this system is about 140%. Losses are in the UV (due to transitions from the $^1S_0$ state to states below the $^1I_6$ state) and in the IR (due to emissions from the $^3P_0$ state to states above the $^3F_3$ state). Already in the mid-70s a lot of compounds (mostly fluorides) doped with Pr^{3+} were tested on their quantum cutting properties [7–9]. Some compounds, like LaF_3, showed $^1S_0$ emissions but others, like $LiYF_4$, did not. In the latter group, the onset of the 4f5d levels is positioned below the $^1S_0$ level and thus 4f5d emissions were observed (see Fig. 1) [10]. The position of the 4f5d levels of rare earth ions is strongly dependent on the properties of the host lattice, like covalency and coordination number. Recently, $^1S_0$ emission of Pr^{3+} was also observed in some oxydic host lattices like $SrAl_{12}O_{19}$ [4], LaB_3O_6 [5] and $LaMgB_5O_{10}$ [6] by Srivastava et al.

For CaF_2 doped with Pr^{3+} contradictory results are presented in the literature. Sommerdijk et al. [8] report that this compound does not show $^1S_0$ emission of Pr^{3+}, while Piper et al. [9] report both 4f5d and $^1S_0$ emissions. Levey et al. [11] observed that the relative intenisty of the $^1S_0$ emission increased for higher Pr^{3+} concentrations and assigned the $^1S_0$ emission to Pr^{3+} cluster sites. High resolution absorption spectra measured by Szczurek and Schlesinger [12] of rare earth doped CaF_2 fluoride crystals show the onset of Pr^{3+} 4f5d bands to be at 223.6 nm, below the $^1S_0$ level. This would mean that no $^1S_0$ emission from Pr^{3+} is possible in CaF_2. However, it is generally known that CaF_2 doped with trivalent rare earth ions gives rise to different sites for the dopant ions (see e.g. Refs. [13–15]). The reason for this is that the trivalent dopant ion replaces a divalent Ca^{2+} ion in the lattice. Charge compensation is thus required and this can be achieved in several ways, leading to sites with different local symmetry and crystal field. The spectroscopy of the intraconfigurational 4f transitions of Pr^{3+} ions on different sites depend in a subtle way on the surroundings and usually high resolution spectroscopy and time-dependent measurements are required to distinguish between the different sites (see e.g. Ref. [15]).

The distribution of Pr^{3+} ions over different sites and the presence of clusters will depend very much on the synthesis conditions, like cooling rate [13] and on the Pr^{3+} concentration. Since the 4f5d transitions are more strongly influenced by the surroundings of the ion, it is expected that the contradicting results presented in literature can be explained by the different coordinations of Pr^{3+} on different sites in CaF_2. In this article, we show that this is the case. Three different sites are observed by selective excitation in 4f5d bands. For identification f–f emissions and f–f lifetimes (after selective fd excitation) are compared with data from the literature [15].

2. Experimental

A crystal of CaF_2 doped with 0.05 mol% of Pr^{3+} was prepared from CaF_2 and PrF_3 in a glassy carbon crucible in a high frequency furnace. The reaction chamber was flushed with ultra pure nitrogen (<0.5 ppm O_2) and heated up to 350°C for more than 12 h to remove water. Then, the temperature was raised to 550°C and SF_6 was flowed through the reaction chamber for half an hour to remove traces of oxygen [16]. Again under N_2, the sample was heated above the melting temperature. The melt was slowly cooled to room temperature and a transparent single crystal was obtained. For measurements, freshly cleaved pieces of this crystal were used.

Excitation and emission spectra were recorded on a Spex 1680 spectrofluorometer, equipped with 0.22 m double monochromators. This apparatus was adapted for VUV excitation measurements. The excitation source was a D_2-lamp (Hamamatsu L1835, 150 W) fitted with a MgF_2 window. The gratings of the excitation monochromator were blazed at 150 nm, the gratings of the emission monochromator at 500 nm. The lamp housing, the excitation monochromator and the sample chamber were flushed with nitrogen for several hours before doing measurements to avoid absorption of VUV radiation by oxygen. Emission spectra in the range 250–750 nm were recorded using a cooled Hamamatsu R928 photomultiplier tube and in the range 200–300 nm using a cooled Hamamatsu R166 photomultiplier tube (solar blind). In the latter range, the emission monochromator was scanned in second order to match the blaze angle of the emission monochromator for a higher throughput. The emission spectra recorded with the R928 PM tube were corrected for the wavelength dependence of the grating efficiency and the detector response using correction spectra provided by the manufacturer. For emission spectra recorded with the R166 PM tube, no such spectra are available. Excitation spectra were recorded in the range 145–350 nm. Excitation spectra were using sodium salicylate excitation spectra. The temperature of the sample could be varied between LHeT and room temperature using an Oxford Instruments Optistat$^{CF\text{-}V}$ liquid helium cold finger cryostat equipped with MgF_2 windows. The maximal spectral resolution of this set-up was about 0.5 nm.

Luminescence decay times were measured using the frequency doubled signal of a Lambda Physik LPD 3000 dye laser at 221 nm with Coumarin 120 as laser dye. The dye laser was pumped by a Lambda Physik LPX excimer laser (XeCl). The signal was detected using an Arc Spectro Pro® o-300i monochromator and a RCA C31034 photomultiplier tube. The decay times were measured using a Tektronix 2440 digital oscilloscope. The sample was cooled in an Oxford Instruments OptistatCF-V liquid helium cold finger cryostat equipped with quartz windows.

3. Results and discussion

Fig. 2 presents a low temperature emission spectrum of a CaF_2 crystal doped with 0.05 mol% Pr^{3+} upon excitation at 177 nm. Strong $^1S_0$ emissions are observed at circa 400 nm ($^1S_0 \rightarrow {}^1I_6$ transition), 336 nm ($^1S_0 \rightarrow {}^1D_2$ transition) and at 274 nm ($^1S_0 \rightarrow {}^1G_4$ transition). The $^1S_0 \rightarrow {}^3F_4$ transitions are observed at about 253 nm using a solar blind PM tube. In the visible part of the spectrum, emissions are ascribed to transitions from the $^3P_0$ state to lower states (see Fig. 2) and to $^1D_2$ emissions (weak, around 600 nm). When the sample is excited at 221 nm at low temperature, the emission spectrum presented in Fig. 3 is obtained.

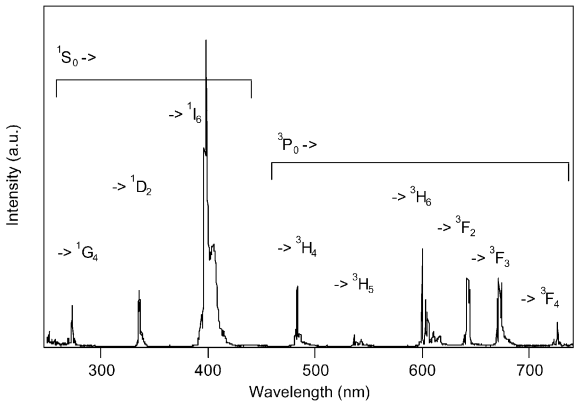

Fig. 2. Emission spectrum of a $CaF_2:Pr^{3+}$ (0.05%) crystal for $\lambda_{exc} = 177$ nm (Pr^{3+} $^3H_4 \rightarrow 4f^15d^1$ transition) at $T = 6$ K.

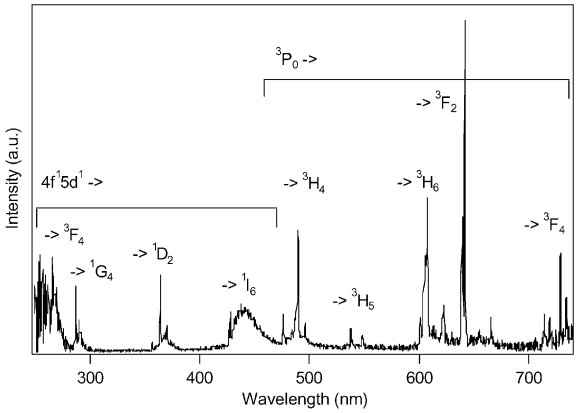

Fig. 3. Emission spectrum of a $CaF_2:Pr^{3+}$ (0.05%) crystal for $\lambda_{exc} = 221$ nm (Pr^{3+} $^3H_4 \rightarrow 4f^1$ $5d^1$ transition) at $T = 6$ K.

Here, no $^1S_0$ emissions are observed, but instead in the UV and blue part of the spectrum 4f5d emissions from Pr^{3+} are observed. The 4f5d emissions appear as zero phonon lines with on the lower energy side some sharp vibronics, superimposed on a broad vibronic side band. Fine structure is not often observed in the 4f5d luminescence spectra of trivalent lanthanides. The presently observed fine structure in the fd emission spectra of Pr^{3+} in CaF_2 is in agreement with the observation of fine structure in the 4f5d excitation spectra of trivalent lanthanides in CaF_2 [12] and is due to the restricted relaxation in the 4f5d excited state for rare earth ions in CaF_2. The assignment of the bands is given in Fig. 3. For the band around 440 nm it is not possible to make a unique assignment, since in this region the $4f5d \rightarrow {}^1I_6$ and the $4f5d \rightarrow {}^3P_{0,1,2}$ emissions will overlap. Probably, the emission bands corresponding to transitions to the ^3P_J levels will be stronger because the lowest 4f5d state is a triplet state. Even though the spin selection is largely lifted for transitions on lanthanides ions due to the strong spin–orbit coupling, it is often observed that formally spin-allowed transitions are stronger than spin-forbidden transitions. Also note that the integrated emission intensity of the $^3P_0$ emissions lines seems to be stronger than the intensity of the $4f5d \rightarrow {}^3P_{0,1,2}$, $^1I_6$ emission band. This has not been analyzed in detail. However, if the $^3P_0$ emission is indeed stronger, this would indicate that there is also direct (nonradiative) relaxation from the 4f5d excited state to the ^3P_J and $^1I_6$ levels, inaddition to population of these levels by radiative decay from the 4f5d state. By making use of a solar blind PM tube, emission spectra have been recorded in the range 200–300 nm. Upon 215 nm excitation, the spectrum of Fig. 4 was obtained. The assignment of the 4f5d bands is given in Fig. 4. All positions of the first zero phonon lines and additional sharp lines are given in Table 1. Similar emission spectra are obtained upon excitation at 150 nm.

The excitation spectrum of the $^1S_0 \rightarrow {}^1I_6$ emission at 403 nm is presented in Fig. 5. As seen from this figure, the onset of the 4f5d band is positioned around 200 nm, which is at higher energy than the position of the $^1S_0$ level (expected around 212 nm).

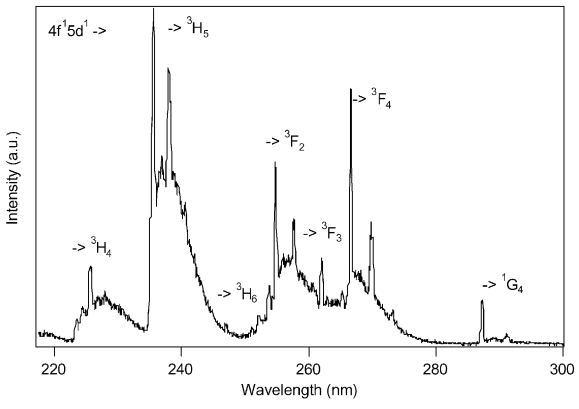

Fig. 4. Emission spectrum of a $CaF_2:Pr^{3+}$ (0.05%) crystal for $\lambda_{exc} = 215$ nm (Pr^{3+} $^3H_4 \rightarrow 4f^1$ $5d^1$ transition) at $T = 6$ K, recorded with a Hamamatsu R166 Solar Blind PM tube.

Table 1
Positions of the first zero phonon line and additional sharp lines (some vibronic, some to higher crystal field components of the $4f^2$ levels) for $4f5d \rightarrow 4f^2$ emissions of Pr^{3+} in $CaF_2:Pr^{3+}$ 0.05% (see Figs. 3 and 4)[a]

$4f^2$ level	Zero phonon line at onset	Other sharp lines	ΔE
$^3H_4$	44743	44543	200
		44307 (s)	436
		43879	864
$^3H_5$	42445	42212	233
		42026 (s)	419
		41580	865
$^3H_6$	40502		
$^3F_2$	39833	39651	182
		39494	339
		39409 (s)	424
		39254 (s)	579
		38812	1021
$^3F_3$	38373	38168 (s)	205
		38052	321
$^3F_4$	37686	37510 (s)	176
		37058	628
		36630	1056
$^1G_4$	34828	34358	455
$^1D_2$	28027	27427	600
		27144	883
		26969	1058
^3P_J, $^1I_6$	23408	23332	76

[a] ΔE gives the energy difference with the zero phonon line at the onset. The error in the positions is relatively large ($\sim 50\,cm^{-1}$) since the spectra were recorded with a VUV adapted Spex Fluorolog with a resolution of about 0.3 nm. Stronger lines are indicated by (s). All values are in cm^{-1}.

The transition to the $^1S_0$ level itself is not observed in this excitation spectrum: it is too weak due to the forbidden character of the intraconfigurational $4f^n$ transition: the overlap with the parity allowed fd absorption band of other Pr^{3+} sites in the same spectral region prevents the observation of the weak parity forbidden transition to the $^1S_0$ level. The 4f5d band consists of several bands: at least four broad and intense bands can be discerned. Their peak positions are 157, 165, 178 and 192 nm.

The excitation spectrum of the $4f^15d^1 \rightarrow {}^3P_{0,1,2}$, $^1I_6$ emission (442 nm) is given in Fig. 6. This spectrum is very different from the spectrum in Fig. 5. Several bands are observed. The first band shows vibrational structure, but the signal is noisy due to the low intensity of the signal. Its first sharp maximum is positioned at 221.3 nm. The bands peaking at 190 and 203 nm are structureless and of a similar intensity as the first band. At 163 nm is the onset of a broad excitation band with high intensity. Fig. 7 presents an excitation spectrum for the $4f^15d^1 \rightarrow {}^1D_2$ emission at 365 nm. This

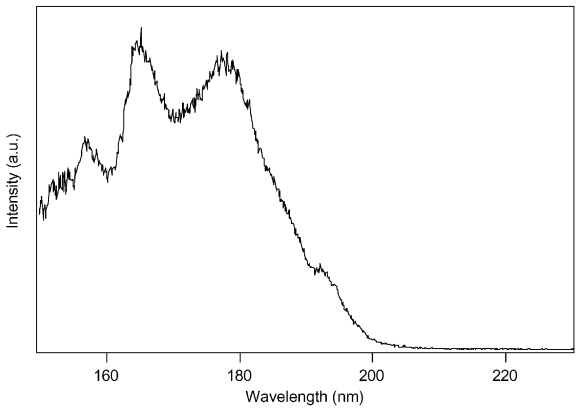

Fig. 5. Excitation spectrum of a $CaF_2:Pr^{3+}$ (0.05%) crystal monitoring emission at 403 nm (Pr^{3+} $^1S_0 \rightarrow {}^1I_6$ transition) at $T = 6$ K.

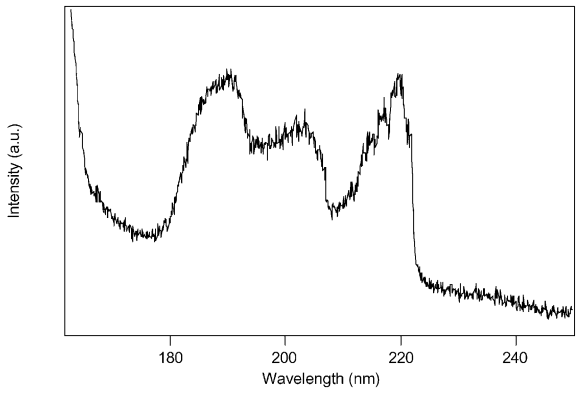

Fig. 6. Excitation spectrum of a $CaF_2:Pr^{3+}$ (0.05%) crystal monitoring emission at 442 nm (Pr^{3+} $4f^1$ $5d^1 \rightarrow {}^1I_6$ transition) at $T = 6$ K.

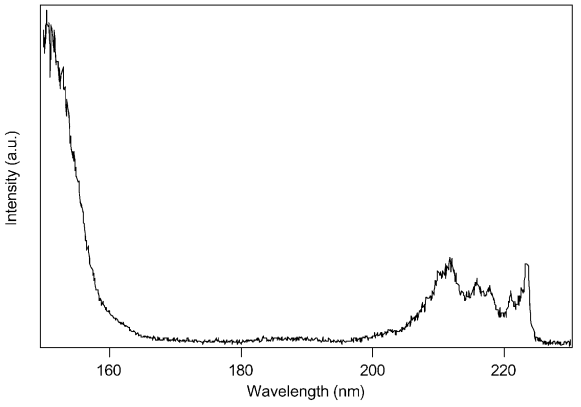

Fig. 7. Excitation spectrum of a $CaF_2:Pr^{3+}$ (0.05%) crystal monitoring emission at 365 nm (Pr^{3+} $4f^1\,5d^1 \rightarrow {}^1D_2$ transition) at $T = 6$ K.

excitation spectrum differs from the $4f^15d^1 \rightarrow {}^3P_{0,1,2}$, $^1I_6$ excitation spectrum. It consists of two broad bands, of which the lower energy band shows fine structure. The zero phonon line is observed at 223.3 nm. At $\pm$165 nm the onset of a broad and structureless band is observed.

Comparison of these results with the absorption spectrum of a crystal of $CaF_2:Pr^{3+}$ (0.05%) as presented by Szczurek and Schlesinger [12] shows some differences and resemblances. The excitation band of the 4f5d emission as presented in Fig. 6 is also found in the absorption spectrum of Szczurek and Schlesinger. Further, they report a zero phonon line at 223.7 nm, which corresponds to the position of 223.3 nm observed in Fig. 7. They also found a broad band, starting at around 200 nm, which is in agreement with the spectrum given in Fig. 5. In absorption spectra, all absorption bands present will be measured, while excitation spectra make it possible to discriminate between different absorption bands form different luminescing centers. Obviously, there are at least three different sets of excitation bands found in our sample, belonging to Pr^{3+} ions on three different types of sites in CaF_2. It is expected that the crystals used in Ref. [12] also contains Pr^{3+} on different sites since the Pr^{3+} concentration and synthesis procedure are very similar. In the remainder of this article, we will comment on these sites and assign two of them to Pr^{3+} sites previously identified on the basis of $f^2 \rightarrow f^2$ emission spectra.

An overview of possible sites in CaF_2: Pr^{3+} is given in an article by Tissue and Wright [15]. In this article, 22 different sites for Pr^{3+} in CaF_2 are described. Three of them are identified as single ion sites. These are the O_h site, the C_{4V} site and a so-called L site (described as a site of low symmetry). The other 19 sites are formed by clusters of two or more Pr^{3+} ions. The sites are identified by the characteristics of the intraconfigurational $4f^2$ emissions. Based on the emission wavelengths, the number of lines in a certain multiplet and the decaytime of the emissions it is possible to discriminate between spectroscopic properties of Pr^{3+} ions on different sites. To identify different sites of Pr^{3+} in our CaF_2 crystal, emission spectra of intraconfigurational $4f^2$ transitions were recorded upon selective excitation in the different sets of 4f5d bands. By comparing these emission spectra with the spectra given in Ref. [15], it is possible to identify the different sites. In Fig. 8 emission spectra of $^3P_0 \rightarrow {}^3H_4$ transitions are presented for two different excitation wavelengths. Clearly, two different emission spectra are obtained. Following the assignment of Tissue and Wright, the upper spectrum is assigned to transitions of a Pr^{3+} ion on an L site, while those of the lower spectrum can be attributed to a Pr^{3+} ion on a C_{4V} site. The number of peaks, their relative intensities and positions are all in agreement with literature data for the L site and the C_{4V} site. Only the resolution of our spectra is lower than those reported in Ref. [15]. At 220 nm Pr^{3+} ions on two different sites will be excited (see Figs. 6 and 7). It should be noted however, that the intensity of the band with the zero phonon line at 223.3 nm is much lower than the bands with the first sharp maximum at 221.3 nm. It is thus reasonable to assume that excitation at 220 nm mainly excites ions of the latter type. This implies that the 4f5d bands of Pr^{3+} on a C_{4V} site have their onset at about 221.8 nm (half a nanometer before the first maximum), while the 4f5d bands of Pr^{3+} on an L site start at 208 nm. The same results are obtained while monitoring the $^3P_0 \rightarrow {}^3F_2$ emissions (Fig. 9). Also in this case spectral characteristics of Pr^{3+} on the different sites agree with those given in

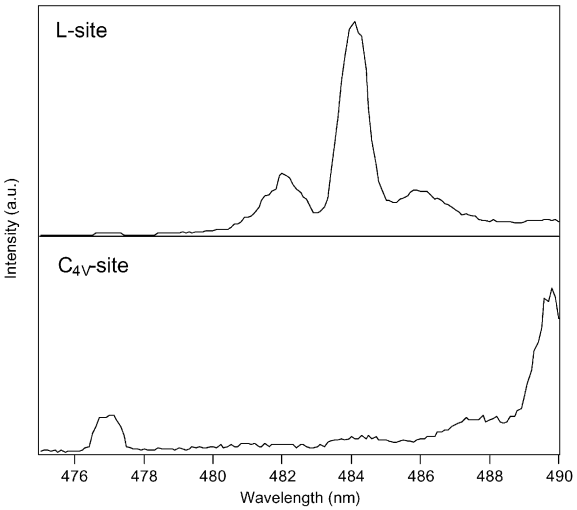

Fig. 8. Emission spectra of $^3P_0 \rightarrow {}^3H_4$ transitions on Pr^{3+} with a resolution of ~ 0.5 nm upon excitation at 177 nm (upper spectrum) and at 220 nm (lower spectrum) at $T = 6$ K.

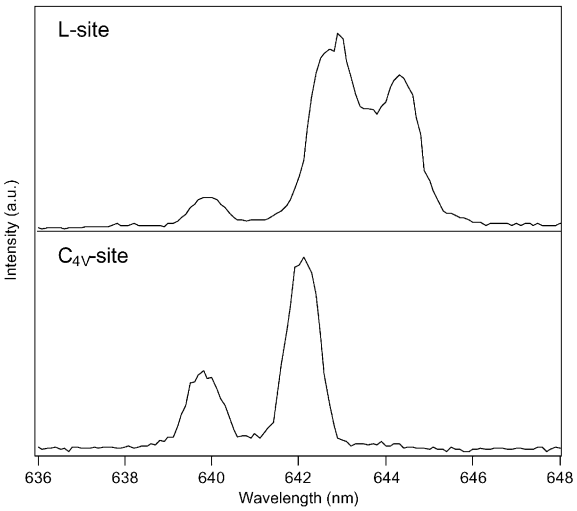

Fig. 9. Emission spectra of $^3P_0 \rightarrow {}^3F_2$ transitions on Pr^{3+} recorded with a resolution of ~ 0.5 nm upon excitation at 177 nm (upper spectrum) and at 220 nm (lower spectrum) at $T = 6$ K.

Ref. [15] for the $^3P_0 \rightarrow {}^3F_2$ emission from Pr^{3+} on the C_{4V} and L site.

The frequency doubled signal of a dye laser (using Coumarin 120 as dye), pumped by an excimer laser, was used to excite selectively in the zero phonon line at 223.3 nm. This yielded an emission spectrum in which only 4f5d bands were observed. Intraconfigurational $4f^2$ emissions were not detected and consequently decay times could not be measured. Thus, the data of Ref. [15] cannot be used to identify this third site. However, the band is tentatively ascribed to Pr^{3+} ions an cubic O site. The symmetry on an O_h site is high and the 4f5d bands are expected to split in only two crystal field components on this site. This is what is observed in Fig. 7. The energy difference between the two bands in the excitation spectrum of Fig. 7 is 21,000 cm^{-1}. This is in good agreement with the crystal field splitting observed for Ce^{3+} on a cubic site in CaF_2 [17,18]. This provides strong support for the assignment to Pr^{3+} on a cubic (distantly charge compensated) site.

The branching ratios of 4f5d emissions to the 4f levels of Pr^{3+} on distinct sites differ significantly from one another. This is concluded from the fact that upon recording an excitation spectrum of a $4f5d \rightarrow {}^3P_{0,1,2}$, $^1I_6$ emission almost only features of the C_{4V} site are observed, while the excitation spectrum of the $4f5d \rightarrow {}^1D_2$ emission shows a different spectrum and is attributed to the excitation spectrum of the O site.

Further support for the assignment described above comes from luminescence lifetime measurements. Upon laser excitation at 221 nm decay times of f–f emissions were recorded. A value of 110 μs for the $^3P_0$ emissions is found. This value is in reasonable agreement with the value of 95.4 ± 4.9 μs as reported in Ref. [15] for the decaytime of the $^3P_0$ emission of Pr^{3+} on a C_{4V} site. The nature of the L site is not clear. In the literature it is mentioned that it is a single ion site of low symmetry [15]. As expected from the low doping concentration, the emission spectra do not give indications for the presence of clusters of Pr^{3+} ions in the crystal.

The results described above explain the findings reported in Refs. [7–9]. In a single crystal of CaF_2: Pr^{3+}, $^1S_0$ emission as well as 4f5d emission can occur, in agreement with the results by Piper et al. [9]. The absence of $^1S_0$ emission in the samples of Sommerdijk et al. [7,8] can possibly be explained

by the absence of Pr^{3+} on sites with a high energy 4f5d onset in their crystals. As mentioned above, the distribution of Pr^{3+} ions over different sites is dependent on concentration and synthesis methods. The absorption spectra presented by Szczurek and Schlesinger [12] show $4f^2 \rightarrow 4f^1 5d^1$ absorption of all different sites.

4. Conclusions

Site selective spectroscopy of the 4f5d bands of different Pr^{3+} sites in CaF_2: Pr^{3+} (0.05%) shows the presence of three different single ion sites. The 4f5d bands of the different sites were identified by comparing the emission spectra upon selective excitation and in case of the C_{4V} site the decay time of intraconfigurational $4f^2$ emissions with results on site selective f–f luminescence spectroscopy for $CaF_2:Pr^{3+}$. The 4f5d bands of Pr^{3+} on a C_{4V} site have their onset at about 221.3 nm. Excitation in these bands yields 4f5d emissions with beautiful fine structure and intraconfigurational $4f^2$ emission from the $^3P_0$ state and from lower states. The 4f5d bands of Pr^{3+} on an L site have their onset at 208 nm. Excitation in these bands yields $^1S_0$ emission, followed by emission from the $^3P_0$ state. A third set of 4f5d bands has its zero phonon line at 223.3 nm. It is suggested that this set of bands belongs to Pr^{3+} on an O_h site. Based on the present results the observation of both $^1S_0$ emission (from Pr^{3+} on the L site) and fd emission (from Pr^{3+} on C_{4V} or O_h sites can be understood.

Acknowledgements

The authors wish to thank Ms. Liesbeth van Pieterson for valuable discussions and practical help. Financial support for this work by Philips Forschungslaboratorien Aachen GmbH is gratefully acknowledged.

References

[1] R.T. Wegh, H. Donker, K.D. Oskam, A. Meijerink, Science 283 (1999) 663.
[2] R.T. Wegh, H. Donker, K.D. Oskam, A. Meijerink, J. Lumin. 82 (1999) 93.
[3] R.T. Wegh, H. Donker, A. Meijerink, R.J. Lamminmaki, J. Holsa, Phys. Rev. B 56 (1997) 13841.
[4] A.M. Srivastava, W.W. Beers, J. Lumin. 71 (1997) 285.
[5] A.M. Srivastava, D.A. Doughty, W.W. Beers, J. Electrochem. Soc. 144 (1997) L190.
[6] A.M. Srivastava, D.A. Doughty, W.W. Beers, J. Electrochem. Soc. 143 (1996) 4113.
[7] J.L. Sommerdijk, A. Bril, A.W. de Jager, J. Lumin. 8 (1974) 341.
[8] J.L. Sommerdijk, A. Bril, A.W. de Jager, J. Lumin. 9 (1974) 288.
[9] W.W. Piper, J.A. DeLuca, F.S. Ham, J. Lumin. 8 (1974) 344.
[10] K.H. Yang, J.A. DeLuca, Phys. Rev. B 17 (1978) 4246.
[11] C.G. Levey, T.J. Glynn, W.M. Yen, J. Lumin. 31&32 (1984) 245.
[12] T. Szczurek, M. Schlesinger, in: B. Jezowska-Trezbiatowska, J. Legendziewicz, W. Strek (Eds.), Rare Earth Spectroscopy, World Scientific, Singapore, 1985, p. 309.
[13] M.J. Weber, R.W. Bierig, Phys. Rev. 134 (1964) A1492.
[14] U. Ranon, W. Low, Phys. Rev. 132 (1963) 1609.
[15] B.M. Tissue, J.C. Wright, Phys. Rev. B 36 (18) (1987) 9781.
[16] M. Robinson, J. Cryst. Growth 75 (1986) 184.
[17] W.J. Manthey, Phys. Rev. B 8 (1973) 4086.
[18] E. Loh, Phys. Rev. 154 (1967) 270.